Bulletin of the Seismological Society of America. Vol. 67, No. 3, pp. 863–876. June 1977

A GENERALIZED STRONG-MOTION ACCELEROGRAM BASED ON SPECTRAL MAXIMIZATION FROM TWO HORIZONTAL COMPONENTS

By J. Shoja-Taheri and Bruce A. Bolt

ABSTRACT

A new form of strong-motion accelerogram ("spectrally maximized record" or "SMR") and its associated generalized spectrum are proposed for earthquake engineering use. Parameters (e.g., spectral, duration, peak amplitude) of strong-motion records at a given site generally depend significantly on the (arbitrary) azimuthal component, sometimes leading to a crucially deficient description of these parameters if only a single component is used. In this paper, combination of horizontal components using spectral maximization is shown to be effective in minimizing the difficulty. The spectra of the two horizontal components at each site are combined to maximize the resultant spectrum, independently of azimuthal orientation. SMR's of 33 important strong-motion accelerograms (including some New Guinea records) are then calculated from their corresponding spectra. In only 60 per cent of cases is the peak acceleration from a maximized spectrum greater than that of the single components. The bracketed duration from the maximized spectrum is always greater. After filtering to provide records in ten frequency bands (0–1 Hz, 1–2 Hz, $\cdots$, 9–10 Hz), correlations for each band are made between acceleration peaks, spectral energy, magnitudes, and source distances. Reasonably stable estimates of strong-motion parameters appear to be given by spectrally maximized seismograms.

Introduction

Major seismological work on determining and defining strong-motion parameters that are stable, i.e., not seriously dependent on abnormal values, is still much needed. Such robust parameters are required for not only purely seismological purposes on understanding earthquake waves (e.g., Bolt, 1972), risk mapping (e.g., Algermissen and Perkins, 1976) and so on, but are vital for engineering design purposes (e.g., Housner, 1970; Newmark and Rosenblueth, 1971). The aim of the present paper is to report some pertinent results of analysis of a variety of strong-motion records. In this search for stable parameters, a new procedure of combining ground motions has been found that may have wide application.

In practice, even in some of the most recent work (e.g., Cloud and Perez, 1969; Schnable and Seed, 1973; Trifunac and Brady, 1975), generally raw measurements of such parameters as peak acceleration have been used for correlations with intensity, magnitude, and distance. The question is whether these parameters would be more robust if spectral characteristics such as frequency and phase were involved. An affirmative answer is likely, because the responses of both complex geological and man-made structures are dominated by seismic-wave characteristics in restricted bands of frequencies. Overall, therefore, the work is directed toward determining the functional dependence of the kinematical parameters on frequency as an independent variable. More specifically, a review of published analyses of strong-motion records and their engineering use shows that the usual procedure is to work separately with wave amplitudes or spectra from just one horizontal component (or the vertical

component) of the ground motion. Because three components are recorded, the problem is to develop a physically acceptable method whereby optimum use is made of all components of strong-motion acceleration, velocity, and so on. The second purpose here, therefore, is to demonstrate the effectiveness of one technique of combining the two horizontal components before parameterization begins. It is suggested that the method, called *spectral maximization*, might be adopted generally with advantage by seismologists and earthquake engineers.

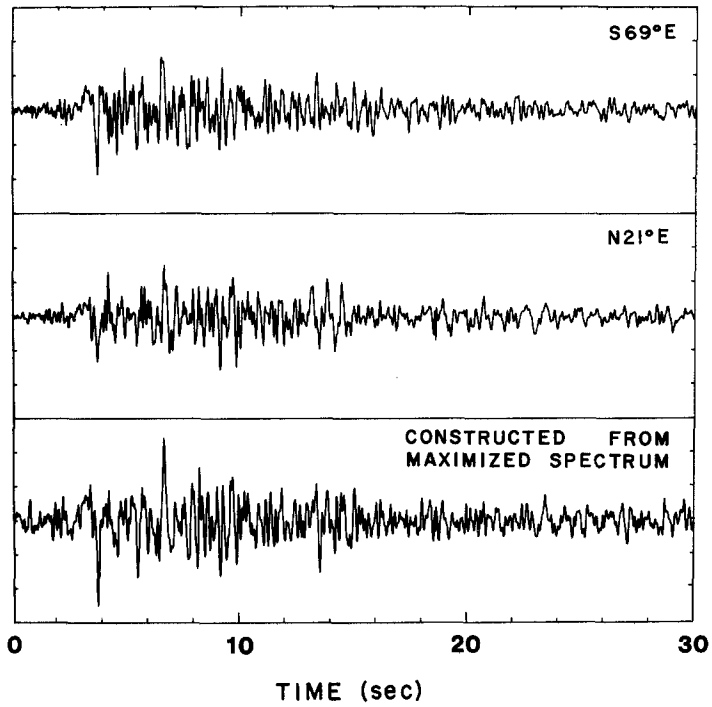

FIG. 1. Horizontal components and their corresponding spectrally maximized accelerogram records (SMR) at Taft in the July 21, 1952 Kern County, California earthquake. One vertical scale division represents 0.1 g.

SPECTRAL MAXIMIZATION

Consider the two orthogonal horizontal components of acceleration recorded at small distances from the earthquake source. These are generally made up of the superposition of many wave types radiating from an areally distributed and moving source—not a single point. The examples shown at the *top* of Figure 1 are the horizontal components (S69°E and N21°E) recorded at Taft in the 1952 earthquake (magnitude 7.7). The directions of instrumental orientation are not related to the strike of the rupturing fault and have no seismological significance. The peak accelerations on the two components are 0.18 g and 0.17 g, respectively. As the seismograms show, these maximum amplitudes occur at quite different times during the motion and give little idea of the result of any vectorial combination.

From the point of view of representing an average earthquake excitation, it is not usually appropriate, at least in the near-field of an earthquake, to resolve the motions in a particular direction. At a site near an earthquake source, such as a rupturing fault, seismic waves of various types, from various foci, traveling various paths in

the crustal rocks, are superimposed in a complicated way. Penzien and Watabe (1975) deal with this problem completely in the time domain by defining a set of orthogonal directions (for 3 components) for which the variances of the component ground motions have stationary values.

We approach the solution quite differently. After numerical trials with many records, we find that one particular combination of the separate frequency spectra of the two (horizontal) components leads to a spectrum which represents closely the overall variation in motion actually occurring at the site. We call this the maximized (horizontal) spectrum of acceleration for the site and, by the inverse Fourier transform, produce the corresponding time history—or spectrally maximized record

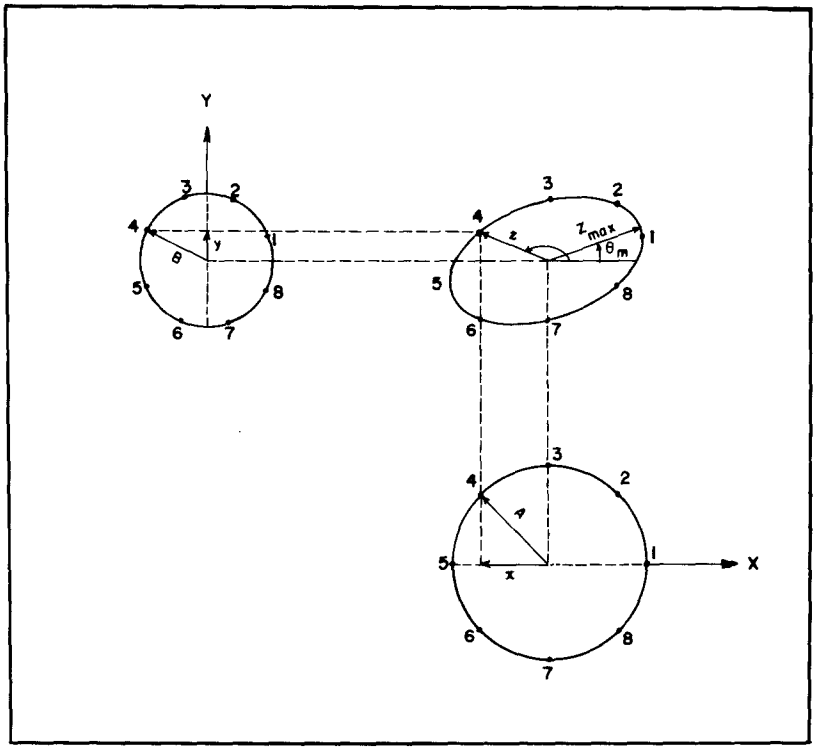

FIG. 2. Method of maximization of the two orthogonal components of ground acceleration for any one spectral frequency.

(SMR). The method differs from that of Penzien and Watabe in the use of the frequency domain and nonstochastic formulation (although statistical interpretation can be given to it).

The method of spectral combination is shown schematically in Figure 2.

Consider the combination of the single-frequency component ω of each of the two horizontal accelerograms orthogonally oriented in the X and Y directions. A vectorial combination of amplitudes (A and B) and phases (ψ_x and ψ_y) can be numerically made so as to produce an elliptical Lissajous figure in the normal way as on an oscilloscope.

The combined acceleration z for a given azimuthal angle θ, from the plus direction, is given by

$$\begin{aligned} z &= x \cos\theta + y \sin\theta \\ &= Z \cos(\omega t + \Phi) \end{aligned} \tag{1}$$

where

$$x = A \cos(\omega t + \psi_x), \tag{2}$$

$$y = B \cos(\omega t + \psi_y). \tag{3}$$

A, ψ_x and B, ψ_y are, respectively, the amplitude and phase of the frequency component ω in the X and Y directions, and Z, Φ are, respectively, the combined amplitude and phase in the θ direction. The combined accelerations, given by (1), define in general an ellipse.

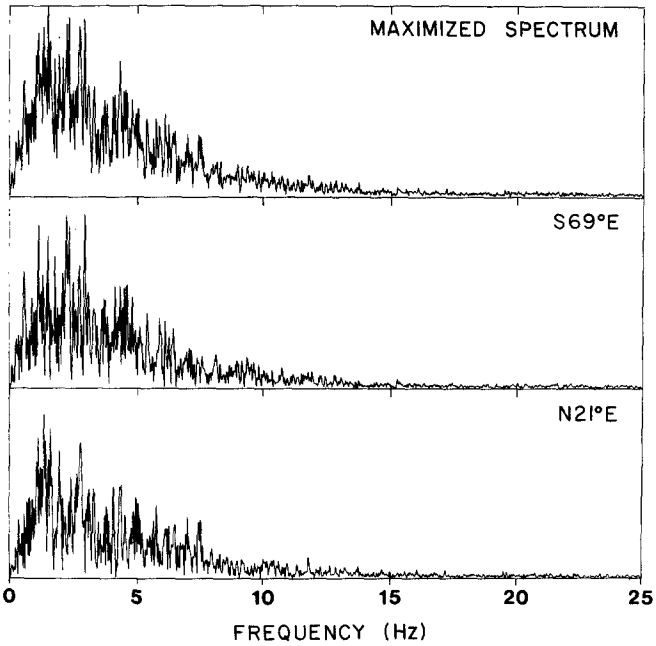

FIG. 3. At the *bottom* are the amplitude spectra for the two orthogonal ground accelerations recorded at Taft in 1952 and shown in Figure 1. At the *top* the maximized spectrum computed from the lower spectra in Figure 1 is compared.

It follows that an angle θ_m can always be found (for the specific frequency ω) such that θ_m is the azimuthal direction of the major axis of the ellipse with respect to the X axis. The combined spectrum given in (1) has maximum amplitude Z_{max} equal to the half-length of the major axis of the ellipse. θ_m is calculated from

$$\theta_m = \tfrac{1}{2} \tan^{-1}((2\ A\ B \cos(\psi_x - \psi_y))/(A^2 - B^2)). \tag{4}$$

Substitution of (4) into (1) yields the *maximized spectrum* as follows

$$z_{max}(\omega) = x \cos\theta_m + y \sin\theta_m = Z_{max} \cos(\omega t + \Phi_{max}). \tag{5}$$

The value of z_{max} is calculated in a computer for each harmonic ω_n, $n = 0, 1, \cdots N$ (N corresponds in the present work to a nyquist frequency of 25 Hz), and the corresponding modulus $| Z_{max}(\omega_n) |$ is plotted.

As an example, Figure 3 compares the maximized spectrum with the two spectra

for the orthogonal horizontal components of the original Taft accelerograms shown in Figure 1. The spectral shape and energy partition with frequency of the original components differ significantly; the maximum energy of the two components clearly occurs in two different frequency bands. It follows that selection of one or other component to describe the motion of the site gives an unrepresentative sample. Similarly, simple vectorial addition of the two-component seismograms toward a specified azimuth would, by introducing an arbitrary parameter, also produce an unrepresentative spectrum. The shape of the maximized spectrum obtained using equation (5) and plotted at the top of Figure 3 is clearly a more satisfactory overall spectral representation of the ground motion.

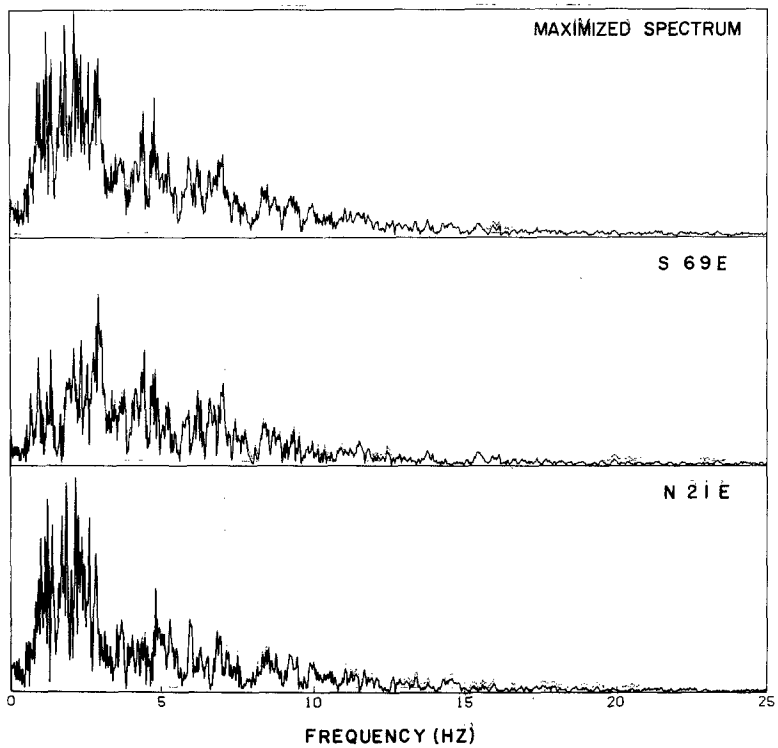

FIG. 4. Amplitude spectra from the recorded horizontal ground accelerations at Castaic Dam in the February 9, 1971 San Fernando, California earthquake. At the *top* is the more representative maximized spectrum for the Castaic site.

Let us now examine the spectrally maximized records (SMR "time histories") obtained by transforming the phases and amplitudes of the maximized spectra to the time domain. Figure 1 compares the actual strong-motion accelerogram from the Taft site in the 1952 earthquake with the corresponding generalized accelerogram (SMR). The SMR for Taft has a peak (horizontal) acceleration of 0.25 g. This illustration is rather typical of the 33 strong-motion records which have been analyzed for the present paper. Consider as a further illustration, the acceleration spectra calculated from the two horizontal strong-motion records at Castaic Dam in the 1971 San Fernando main shock (Richter magnitude 6.5 and source-to-site distance 20 km). The spectral shapes in Figure 4 are strikingly different for the two components, with much more energy between 1 and 3 Hz on the N21°E component. Indeed, selection for structural testing of the S69°E component would significantly underestimate

the shaking at the lower frequencies. In contrast, the maximized spectrum calculated for this site appears to sample without bias the stronger motion on both components.

Fourier transformation of the maximized spectrum at the *top* of Figure 4 yields the spectrally maximized record (SMR) at the *bottom* of Figure 5. Cross correlation by eye of the three accelerograms in Figure 5 suggests at once that the individual records are contained in a general way in the SMR. The latter appears more uniform with less modulation and, on average, with higher amplitudes throughout the shak-

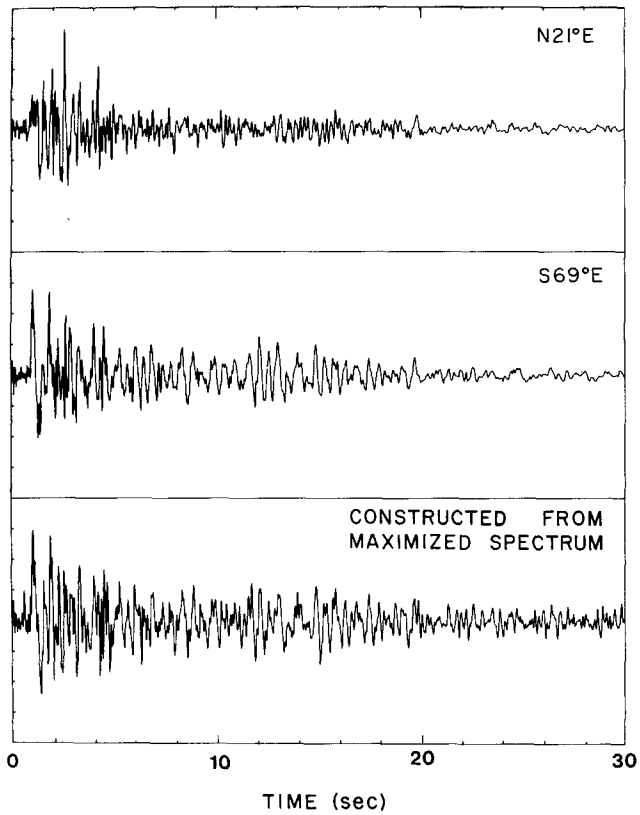

FIG. 5. Recorded horizontal-component accelerograms from Castaic on February 9, 1971 compared with the spectrally maximized accelerogram (SMR). One vertical scale division represents 0.1 *g*.

ing. The SMR is certainly not a simple superposition of the individual components, however; some peaks in the latter are reduced while some are enhanced in the SMR.

We have calculated maximized spectra and SMR for many sites around the world, of which thirty-three are referred to in this analysis (see Table 1). These records come from California, Washington, Japan, Peru and New Guinea (Denham *et al.*, 1973). An overall comparison between the original accelerograms and the corresponding SMR reveals several general properties.

First, in many cases the transformation does not remove the seismic wave pattern on the original components. It is often feasible still to identify certain seismic phases such as *P* and *S*. For example, the onset of the *S*-wave trains can be seen on all records plotted in Figures 1 and 5.

Second, SMR amplitudes are generally, but not always, greater than the ampli-

TABLE 1

STRONG-MOTION RECORDS ANALYZED

No.	Recording Site	Component	Peak Acceleration (cm/sec²)	
			Original	Generalized
1	Vernon, Calif., 3/14/33	N82W	151.0	183.0
		S08W	131.0	
2	El Centro, Calif., 5/18/40	West	215.0	338.0
		South	346.0	
3	Ferndale, Calif., 9/11/38	SE	89.0	132.0
		NE	156.0	
4	Ferndale, Calif., 2/9/41	SE	41.0	56.0
		NE	65.0	
5	Ferndale, Calif., 10/7/51	S44W	118.0	148.0
		N46W	115.0	
6	Ferndale, Calif., 9/22/52	N44E	58.0	99.0
		S46E	75.0	
7	Ferndale, Calif., 12/21/54	N44E	162.0	230.0
		N46W	204.0	
8	Seattle Wash., 4/13/49	SO2W	69.0	81.0
		N88E	67.0	
9	Olympia, Wash., 4/13/49	S86W	284.0	286.0
		S04E	175.0	
10	Eureka, Calif., 12/21/54	N79E	272.0	298.0
		N11W	164.0	
11	Taft, Calif., 7/21/52	S69E	185.0	248.0
		N21E	155.0	
12	Golden Gate Park, Calif., 3/22/57	S80E	102.0	117.0
		N10E	103.0	
13	Olympia, Wash., 4/29/65	S04E	146.0	201.0
		S86W	199.0	
14	Temblor, Calif., 6/27/66	S25W	363.0	
		N65W	265.0	377.0
15	Cholame-Shandon, Calif., No. 5, 6/27/66	N05W	371.0	284.0
		N85E	424.0	
16	Cholame-Shandon, Calif., No. 8, 6/27/66	N50E	219.0	234.0
		N40W	260.0	
17	Cholame-Shandon, Calif., No. 12, 6/27/66	N50E	61.0	75.0
		N40W	64.0	
18	Castaic Old Ridge, Calif., 2/9/71	N21E	325.0	290.0
		S69E	274.0	
19	Itajima, Japan, 1968	N74E	436.0	371.0
		N16W	362.0	
20	Hiroo, Japan, 1970	NS	402.0	461.0
		EW	412.0	
21	Lima, Peru, 3/31/70	N13W	122.0	147.0
		N103W	126.0	
22	Yonki, New Guinea, 11/14/67	HA*	46.0	46.0
		HB	46.0	
23	Rabaul, New Guinea, 10/01/71	HA	61.0	69.0
		HB	68.0	
24	Yonki, New Guinea, 6/17/68	HA	30.0	34.0
		HB	38.0	
25	Yonki, New Guinea, 3/10/69	HA	38.0	33.0
		HB	30.0	
26	Yonki, New Guinea, 5/13/70	HA	25.5	31.9
		HB	30.2	

Table 1—*Continued*

TABLE 1—*Continued*

No.	Recording Site	Component	Peak Acceleration (cm/sec²)	
			Original	Generalized
27	Yonki, New Guinea, 2/12/71	HA	157.0	206.0
		HB	163.0	
28	Yonki, New Guinea, 2/13/71	HA	78.2	53.2
		HB	46.5	
29	Yonki, New Guinea, 1/19/72	HA	16.5	20.7
		HB	19.8	
30	Panaguna, New Guinea, 9/7/69	HA	58.3	59.3
		HB	42.6	
31	Panaguna, New Guinea, 3/28/70	HA	81.1	138.0
		HB	119.9	
32	Panaguna, New Guinea, 7/26/71	HA	36.3	63.4
		HB	58.5	
33	Panaguna, New Guinea, 3/10/69	HA	26.4	25.5
		HB	20.3	

* See Denham *et al.* (1973).

tudes at the same epoch on the separate components. In Table 1, peak accelerations of thirty-three sets of horizontal components and peak accelerations of corresponding generalized records are shown. The peaks of the generalized SMR are higher, in a majority of cases (60 per cent), than the peaks of original components. The greatest enhancement of a peak acceleration occurs for the Taft accelerograms (Figure 1) where it amounts to 35 per cent. Of special interest, because of their wide use for engineering design, the two horizontal components at El Centro in the May 18, 1940 Imperial Valley earthquake yield an SMR with a peak acceleration of 0.34 g, which is slightly but not significantly less than the peak of the observed South component.

Third, there is a uniform pattern in the duration of the spectrally maximized records. Let us consider the bracketed duration (Bolt, 1973), i.e., the elapsed time (for a specified frequency range) between the first and last acceleration excursions on the record greater than a given amplitude level (say, 0.05 g). We find that, as might be expected, for all 33 cases analyzed, the bracketed durations of the SMR's are greater than those of the components. The increase ranges up to 10 per cent. We conclude that, when considering the overall shaking at a site, maximum duration should be measured from the spectrally maximized record rather than from the individual components.

Estimates of Strong-Motion Parameters

In this section, all measurements will be made from the frequency spectra and accelerograms derived by the spectrally maximized method outlined above. The aim is to investigate significant tendencies of strong ground motion when the motion is represented by the SMR at each site rather than separate orthogonal components.

It has already been pointed out in numerous studies (e.g., Bolt, 1973; Trifunac and Brady, 1975) that the characterization of energetic seismic waves near the source is strongly dependent on the wave frequency. In order to examine the matter further, the 33 SMR for sites listed in Table 1 were filtered through ten sequential frequency bands 0–1 Hz, 1–2 Hz, $\cdots$, 9–10 Hz, using a Butterworth filter with eight poles (Gold and Rader, 1969). These filters provide suitably narrow passbands with, of

course, some phase shifts. A typical result is illustrated in Figure 6 for the 1952 Taft SMR (compare with Figure 1 for an absolute time scale). As is often the case with other observed time histories, the peak acceleration at different frequencies occurs at different epochs. The implication is that the peak acceleration of an unfiltered strong-motion record does not necessarily represent the peak acceleration in all frequency bands.

The important inference therefore emerges that correlations of peak acceleration with other variables (such as intensity and source-to-site distance) might be more stable if they were made as a function of frequency. Let us first consider the outstanding problem of correlations of maximum acceleration with the total intensity of

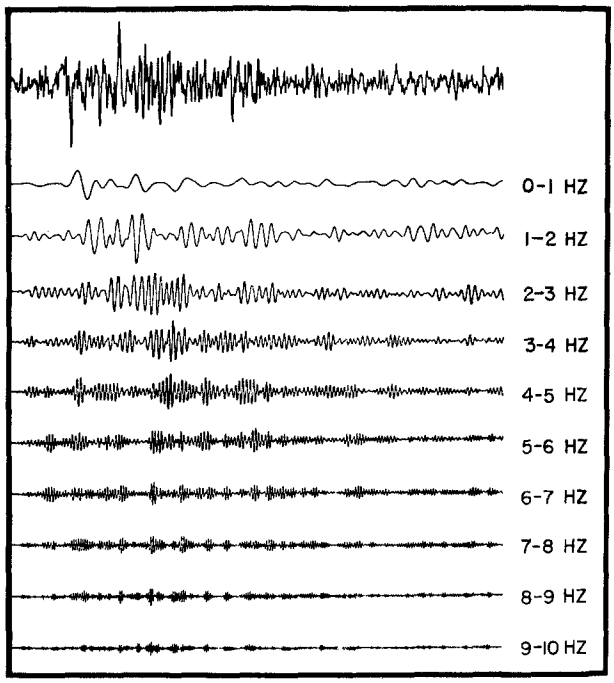

FIG. 6. The generalized accelerogram (SMR) for Taft in 1952 compared with its frequency components obtained by band-pass filtering.

shaking at a site. By Parseval's theorem (Jeffreys and Jeffreys, 1946) the total energy in the time domain equals the integral of the squared amplitude in the frequency domain. (The physical interpretation of the theorem is that the total energy in the traveling waves is the sum of the energies in the normal modes at the site.)

For any band-passed accelerogram $a(t)$, such as those shown in Figure 6, we can therefore write

$$\mathrm{I} = \int_0^T a^2(t)\, dt = \int_{f_1}^{f_2} |\, F(f)\, |^2\, df, \tag{6}$$

where $F(f)$ is the amplitude spectrum and f_1 and f_2 are the lower and upper frequency limits of $a(t)$. If we identify the right-hand-side of (6) with the total "site intensity," then this can be calculated, using the right-hand side, from the maximized spectra for each site. The *normalized peak acceleration*, NPA, for each site is then defined as

$$\mathrm{NPA} = \text{Peak Acceleration}/\mathrm{I}^{1/2} \tag{7}$$

From (6) and (7), normalized peak accelerations for 29 United States and New Guinea records were calculated for each of the ten frequency bands from 1 to 10 Hz. (Japan, Seattle 1949, and Peru records were omitted at this step.) For each frequency band the mean of the 29 normalized peak accelerations was calculated and plotted on Figure 7, together with the standard error of each measurement (not the standard error of the mean).

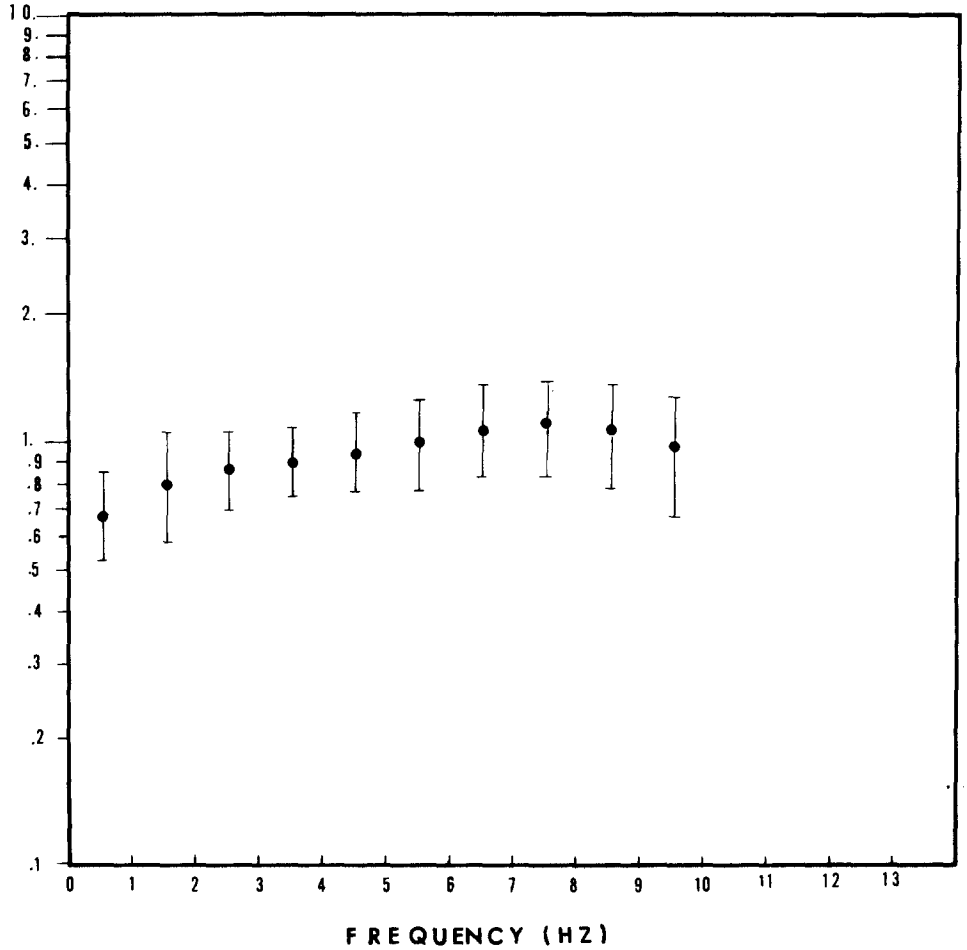

FIG. 7. Means of normalized ratios of peak accelerations (NPA) in different frequency bands SMR's from 29 U.S. and New Guinea strong-motion accelerograms were used to obtain peak values. The bars show the standard errors of one measurement.

Figure 7 shows that the variation of the normalized peak accelerations is relatively small, ranging from 0.7 at the lower frequencies to 1.2 at the higher frequencies. Further, from 4 to 7 Hz, the ratio is stable and not significantly different from unity. Two results of value emerge. First, at least for these observations, there is a close correlation between peak acceleration, as measured by the SMR, and the total intensity of shaking, as defined in (6).

Second, we have obtained an algorithm which permits the estimation of peak acceleration expected for a proposed time history or spectrum of strong ground shaking. Suppose, for example, that several synthetic spectra of ground acceleration are considered for design purposes at a site. The question then may be: What is the maximum

ground acceleration to be expected to correspond to each of them, in a specified frequency range? This mean value can be estimated by calculating I from (6) and then substituting it into (7) together with the appropriate NPA read from Figure 7.

A check on this procedure using the data set of Table 1 is illustrated in Figure 8. For each site, a calculated peak acceleration was obtained for the passband 3–4 Hz multiplying the mean NPA by the appropriate I. These calculated values were then plotted against the peak acceleration actually measured on the filtered SMR. As expected, this reverse process for the present data produces a linear regression with

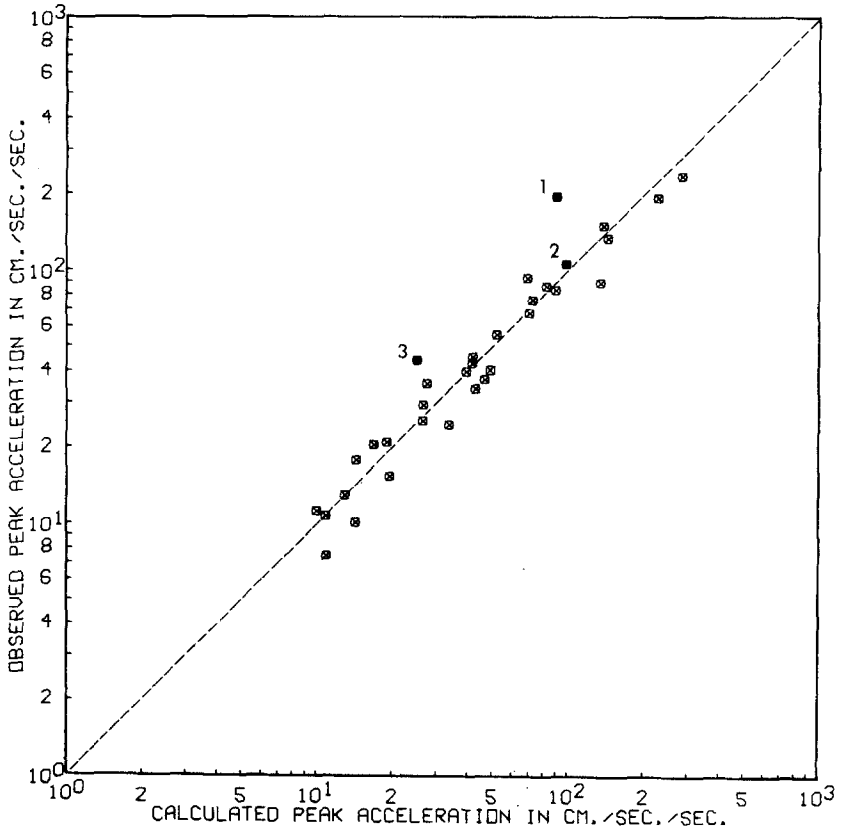

FIG. 8. Observed peak accelerations read from the band-filtered (3–4 Hz) SMR for 33 stations, correlated against the corresponding peak accelerations calculated using equation (7). Points 1, 2, and 3 refer to Temblor (1966), Castaic (1971) and Golden Gate Park (1957), respectively.

generally small scatter. The outlying points marked 1 and 3 on Figure 8 correspond to the 1966 Temblor and 1957 Golden Gate records. At these sites the foundations are rock, which might explain why the predicted values are lower than the observed peak values. On the other hand, point 2 corresponds to the Castaic record also made on rock and its prediction is normal. (The calculated peak accelerations for Temblor and Castaic were actually lower than the observed values for all frequency bands from 1 to 10 Hz.) Prediction for the Peru site is also close.

Finally, we now consider the problem of estimation of attenuation of peak acceleration with distance as a function of frequency. The procedure was to plot the peak accelerations measured from the filtered SMR for each site against the distance between the site and the source. (The nearest point on the offset fault was taken when this was known; otherwise the epicentral distance was adopted.) Two examples of

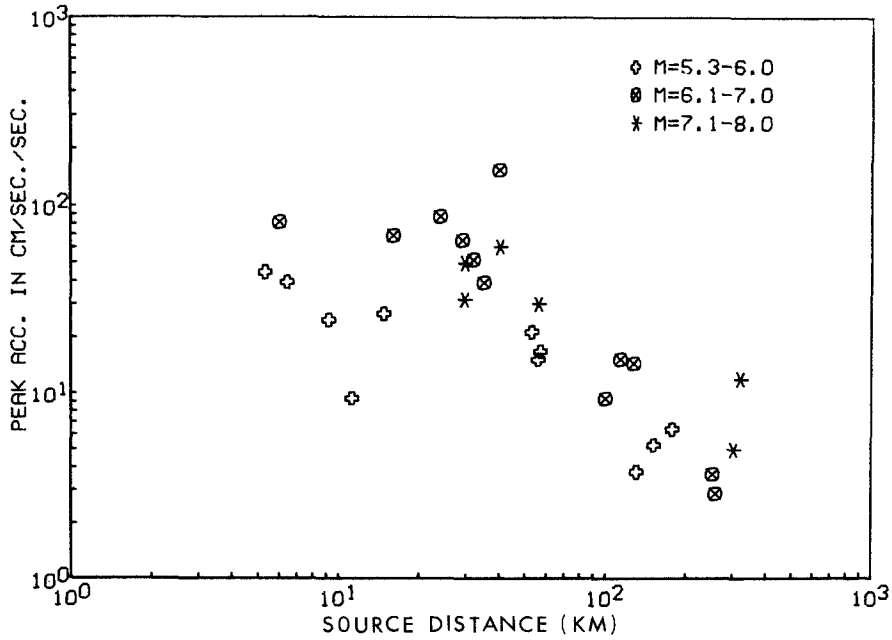

FIG. 9. Regression of the maximum acceleration measured from the 0–1 Hz band-passed generalized accelerograms (SMR) against source distance. Sites 23, 28, 29 and 33 in Table 1 were omitted since source distances are so uncertain.

the regression are shown in Figures 9 and 10. In Figure 9, measurements were made for the waves with frequencies between 0 and 1 Hz and in Figure 10 the case of the 3–4 Hz band is illustrated. The Richter magnitudes of the earthquakes involved are denoted by different symbols.

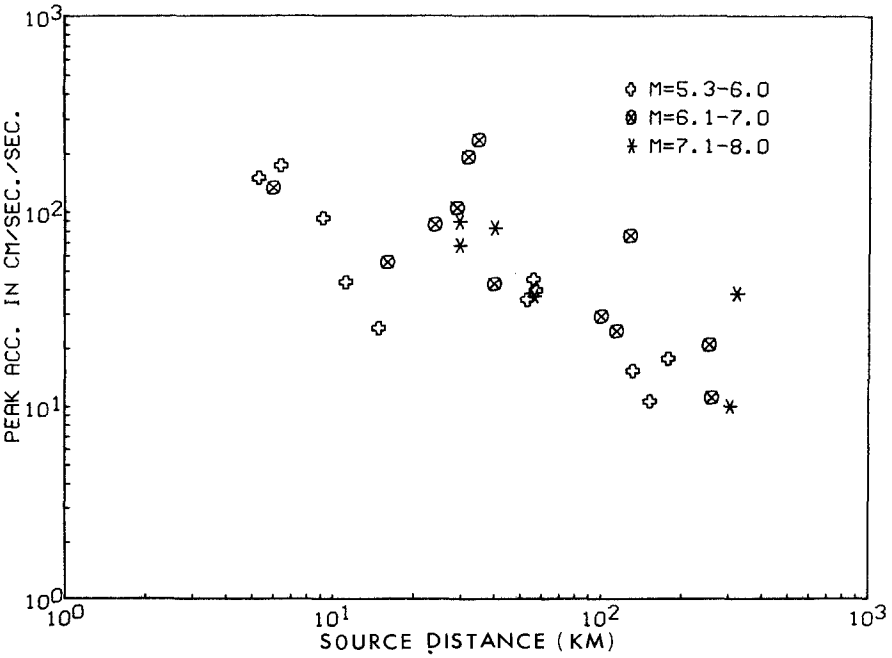

FIG. 10. Regression of the maximum acceleration measured from the 3–4 Hz band-passed generalized accelerograms (SMR) against source distance.

As indicated in Figures 9 and 10, the overall result was a significant tendency for decreased peak acceleration with distance for each frequency band. While the trend is clear, there is some variation at each site from frequency band to frequency band. Many correlations of peak acceleration against source distance have been previously published and some have achieved considerable use in estimation of site parameters and seismic risk (e.g., Cloud and Perez, 1969; Schnabel and Seed, 1973; Donovan, 1974; Algermissen and Perkins, 1976). Most, however, do not consider frequency dependence and use records of the separate components of horizontal ground motion. All published correlations show a high degree of scatter and the fitted mean curves have high uncertainties. The procedures used in this study appear to have reduced the usual scatter somewhat, but considerable dispersion remains, presumably from source path and site effects. An additional feature of interest in the present analysis is that in the separate frequency bands, the plotted points do not clearly separate with magnitude. This is evident on Figures 9 and 10, for example, where Richter magnitudes range from 5.3 to 8.0. The same result was pointed out previously (e.g., Donovan, 1974) and is, in our view, an expected consequence of the modern seismological model of earthquake genesis (Bolt, 1972).

For the sake of comparison with other studies, logarithmic forms $PA = a\Delta^{-b}$ were fitted to attenuation plots, where PA is the peak acceleration and Δ the distance. The least-squares estimates of b have large standard errors when no weighting of observations is used and no clear dependence of b on the frequency band is apparent from the estimations, at least for the sites of strong motion used in this paper, mainly California. Overall, a reasonable fit to the sample points is provided by the attenuation law $PA = a\Delta^{-1/2}$, for $10 < \Delta < 200$ km, and frequencies from 1 to 8 Hz.

Conclusions

The paper introduces a new method of combining individual recorded components of strong ground motion. Combination is accomplished in the frequency domain by spectral maximization at each frequency. The corresponding spectra and accelerograms (spectrally maximized records) appear to have broad representative properties in summarizing the complex shaking at a site. Nowadays, the response of large structures, such as dams, bridges, nuclear reactors and high-rise buildings, is calculated based on seismological estimates of likely ground motion. It is suggested that an SMR would provide a more satisfactory and prudent test of ground motion than a single component of recorded motion.

On the seismological side, analysis of a set of recorded accelerograms with relatively large amplitudes indicates that use of spectrally maximized records at each site allows more stable statistical correlations to be made of key strong-motion parameters such as duration, intensity, peak acceleration and attenuation.

In particular, SMR's allow a clear demonstration of the importance of taking account of the frequency dependence of strong-motion parameters. Indeed, as Figure 6 indicates, a physically advantageous procedure in selecting peak acceleration as a design parameter for a given structure is to use SMR accelerograms with frequency components restricted to the spectral band in which the structure has significant response.

The work has also provided a method of predicting an expected maximum acceleration for any given acceleration amplitude spectrum. At least for the frequency range 4 to 7 Hz, the average peak acceleration and the intensity of shaking seem closely correlated. It would be valuable to extend the calculation of energy over a wider

frequency range when a more extensive set of observed accelerations becomes available.

Examination of the distance attenuation of peak acceleration as a function of frequency indicates that some of the scatter usually observed with raw measurements can be reduced by using SMR's as a function of frequency. Further analysis of the variation must involve geological and source mechanism considerations. Use of the recent records from New Guinea tends to confirm the view that attenuation laws are in general not strongly dependent upon earthquake magnitude. Use of this quantity as a strong scaling parameter on acceleration is not supported by the present analysis.

For the convenience of other workers, punched card decks containing a digital sample of the spectrally maximized accelerograms for the 33 sites listed in Table 1 are available on request to the authors.

Acknowledgments

We would like to thank the Director of the Australian Bureau of Mineral Resources, Geology and Geophysics, for providing the New Guinea strong-motion records used in the present paper.

This research has been financially supported by the National Science Foundation Grant AEN 74-21548.

References

Algermissen, S. T. and D. Perkins (1976). A probabilistic estimate of maximum acceleration in rock in the contiguous United States, *U.S. Geological Survey, Open File Report 76-416*.

Bolt, B. A. (1972). San Fernando rupture mechanism and the Pacoima strong motion record, *Bull. Seism. Soc. Am.* **62**, 1053–1061.

Bolt, B. A. (1973). Duration of strong ground motion, *Proc. World Conference on Earthquake Engineering, Fifth, Rome*, Italy.

Cloud, W. K. and V. Perez (1969). Strong motion—records and acceleration, *Proc. World Conference on Earthquake Engineering, Fourth, Santiago*, Chile.

Denham, D., G. R. Small and I. B. Everingham (1973). Some strong motion seismic results from Papua, New Guinea 1967–1972, Bureau of Mineral Resources, Geology and Geophysics, Australia, *Record 1973/13*.

Donovan, N. C. (1973). A statistical evaluation of strong motion data including the February 9, 1971 San Fernando earthquake, *Proc. World Conference on Earthquake Engineering, Fifth, Rome*, Italy.

Gold, B. and C. M. Rader (1969). *Digital Processing of Signals*, McGraw-Hill, New York, 269 pp.

Housner, G. W. (1970). Strong ground motion, Chapter IV in *Earthquake Engineering*, R. L. Wiegel, Editor, Englewood Cliffs, New Jersey.

Jeffreys, H. and B. S. Jeffreys (1946). *Methods of Mathematical Physics*, Cambridge.

Newmark, N. M. and E. Rosenblueth (1971). *Fundamentals of Earthquake Engineering*, Prentice-Hall, New Jersey.

Penzien, J. and M. Watabe (1975). Characteristics of 3-dimensional earthquake ground motion, *Earthquake Eng. Struct. Dynamics*, **3**, 365–373.

Schnabel, P. B. and H. B. Seed (1973). Accelerations in rock for earthquakes in the Western United States, *Bull. Seism. Soc. Am.* **63**, 501–576.

Trifunac, M. D. and A. G. Brady (1975). A study on the duration of strong earthquake ground motion, *Bull. Seism. Soc. Am.* **65**, 581–626.

Seismographic Station
University of California
Berkeley, California 94720

Manuscript received November 10, 1976